Biomaterials Science

Improvement of DNA recognition through molecular imprinting: hybrid oligomer imprinted polymeric nanoparticles (OligoMIP NPs)

Journal:	*Biomaterials Science*
Manuscript ID	BM-ART-08-2015-000341.R2
Article Type:	Paper
Date Submitted by the Author:	11-Oct-2015
Complete List of Authors:	Brahmbhatt, Heli; The Open University, Life, Health and Chemical Sciences Poma, Alessandro; University College London, Chemistry; The Open University, Life, Health and Chemical Sciences Pendergraff, Hannah; University of Southampton, Chemistry Watts, Jonathan; University of Southampton, Chemistry Turner, Nicholas; The Open University, Life, Health and Chemical Sciences

Biomaterials Science

PAPER

Improvement of DNA recognition through molecular imprinting: hybrid oligomer imprinted polymeric nanoparticles (OligoMIP NPs)

Received 26th August 2015,
Accepted 00th January 20xx

DOI: 10.1039/x0xx00000x

www.rsc.org/

H. Brahmbhatt,[a] A. Poma,*[a,b] H. M. Pendergraff,[c] J. K. Watts[c] and N. W. Turner*[a]

High affinity and specific binding are cardinal properties of nucleic acids in relation to their biological function and their role in biotechnology. To this end, structural preorganization of oligonucleotides can significantly improve their binding performance, and numerous examples of this can be found in Nature as well as in artificial systems. Here we describe the production and characterization of hybrid DNA-polymer nanoparticles (OligoMIP NPs) as a system in which we have preorganized the oligonucleotide binding by molecular imprinting technology. Molecularly imprinted polymers (MIPs) are cost-effective "smart" polymeric materials capable of antibody-like detection, but characterized by superior robustness and the ability to work in extreme environmental conditions. Especially in the nanoparticle format, MIPs are dubbed as one of the most suitable alternatives to biological antibodies due to their selective molecular recognition properties, improved binding kinetics as well as size and dispersibility. Nonetheless, there have been very few attempts at DNA imprinting in the past due to structural complexity associated with these templates. By introducing modified thymine bases into the oligonucleotide sequences, which allow establishing covalent bonds between the DNA and the polymer, we demonstrate that such hybrid OligoMIP NPs specifically recognize their target DNA, and that the unique strategy of incorporating the complementary DNA strands as "preorganized selective monomers" improves the recognition properties without affecting the NPs physical properties such as size, shape or dispersibility.

Introduction

Nucleic acids must bind their targets with high affinity and specificity to play a useful role in biology and biotechnology alike. Structural preorganization of oligonucleotides can improve binding affinity and specificity, and can be achieved in several ways. For example, conformationally locking the sugar ring of nucleotides increases oligonucleotide binding affinity and specificity to such a degree that it has opened up dozens of new opportunities in biotechnology.[1]

Cellular proteins can achieve this preorganization in other ways; e.g., Argonaute proteins prearrange the seed sequence of microRNAs into a helical structure which allows this short sequence to bind its targets with very high affinity.[2]

Thus two very different means of preorganization both lead to the same biological effect – high binding affinity.

In this paper, we describe yet another very innovative method of conformational preorganization - in this case via the artificial molecular recognition method molecular imprinting - that leads to an oligonucleotide-polymer hybrid capable of binding its targets with high affinity.

Unlike ordinary polymers, molecularly imprinted polymers (MIPs) are tailor-made recognition polymers which can be prepared for a variety of targets, ranging from small molecules,[3] to toxins,[4] to proteins,[5] and even bacteria and cells.[6]

Especially in the nanoparticle format,[7] MIPs are dubbed as one of the most suitable alternatives to biological antibodies due to their selective molecular recognition properties, together with increased robustness, improved binding kinetics as well as size and dispersibility.[8]

The integration of nucleic acid with molecular imprinting technology has already been attempted at the macroscale level, with the production of nucleotide imprinted polymeric monoliths or films.[9] The preparation and performance of these bulk polymeric materials, despite being historically significant, is however very tedious and poorly efficient, resulting in polymers which exhibit a distribution of binding sites with non-homogeneous affinity, as well as possible leakage of unwashed template from the material.

A potential strategy to improve the affinity distribution of the binding moieties, as well as to avoid template leakage, is the immobilization of the template molecule onto a suitable solid support,[10] which on a nanoscale level has already proven advantageous to produce MIP NPs exhibiting nanomolar to subnanomolar affinities for specific kinds of targets, also using

[a] Department of Life, Health and Chemical Sciences, The Open University, Milton Keynes, MK7 6AA, United Kingdom. E-mail: n.w.turner@open.ac.uk
[b] Department of Chemistry, University College London, London, WC1H 0AJ, United Kingdom
[c] Department of Chemistry, University of Southampton, Highfield, Southampton, SO17 1BJ, United Kingdom

automatic reactors.11 Nonetheless, even if these imprinted nanomaterials are more suitable to mimic the actual antibody proteins,[8] their composition is still based on the same "classic" monomers which have been used for the past 30 years to produce bulk MIPs, definitely not tailored for the specific target molecule. As a result, when considered against the breadth of molecular imprinting research, materials that target DNA as a template are in a significant minority.

To try addressing this issue, in our previous work we have introduced chemically modified nucleobases (complementary to the template) into the polymer composition used during the solid-phase synthesis of the MIP NPs. We found that the incorporation of such "polymerizable nucleosides" results in an overall improved recognition performance in comparison to the MIP NPs lacking this modification.[12] We have also demonstrated that an aptamer sequence can be incorporated into a MIP NP to yield a nanoparticle with specific, high-affinity binding of a small molecule target.[13] Given that these "hybrid" materials utilize a ssDNA sequence as the recognition element, the use of them to bind specific sequences of ssDNA was an obvious area to investigate.

As a consequence, here we present the first hybrid oligonucleotide-polymer system (OligoMIP NPs) designed to recognize a complementary strand, wherein polymeric NPs have been imprinted for the recognition of the 12mer sequence 5'-AGC TAG CTA GCT-3' as a model oligonucleotide template. The opportunities that could be afforded by such nanoparticulate recognition elements capable of selective binding to a known sequence are very interesting in the fields of bioanalytical chemistry. In addition, the methodology described here has the potential to overcome the heterogeneity problems observed in prior attempts at molecular imprinting using DNA as a target, and which have hindered the broad applications of MIPs as DNA recognition systems.

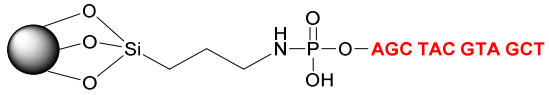

Fig. 1 Schematic of the template DNA sequence (5'-AGC TAG CTA GCT-3') immobilized through the 5'-phosphate group.

Results and discussion

The template DNA sequences have been immobilized on 75 µm glass beads as solid support by 1-ethyl-3-(3-dimethylaminopropyl)carbodiimide (EDC)-mediated amine coupling to the 5'-phosphate group of the DNA sequences (Fig. 1).[14]

Then, the complementary oligonucleotide sequences (i.e. 5'-AGC TAG CTA GCT-3') or control sequences have been allowed to attain thermodynamic equilibrium with the immobilized template strand through non-covalent interactions. These "monomer" sequences have been chemically synthesized either by using 5'-phosphate-linked Acrydite™ modifications,[15] or by introducing C-5 alkene-modified 2'-deoxyuridine residues into the DNA strand,[12] thus resulting in single or multiple covalent anchoring points between the oligonucleotide and the polymer matrix (Fig. 2a).

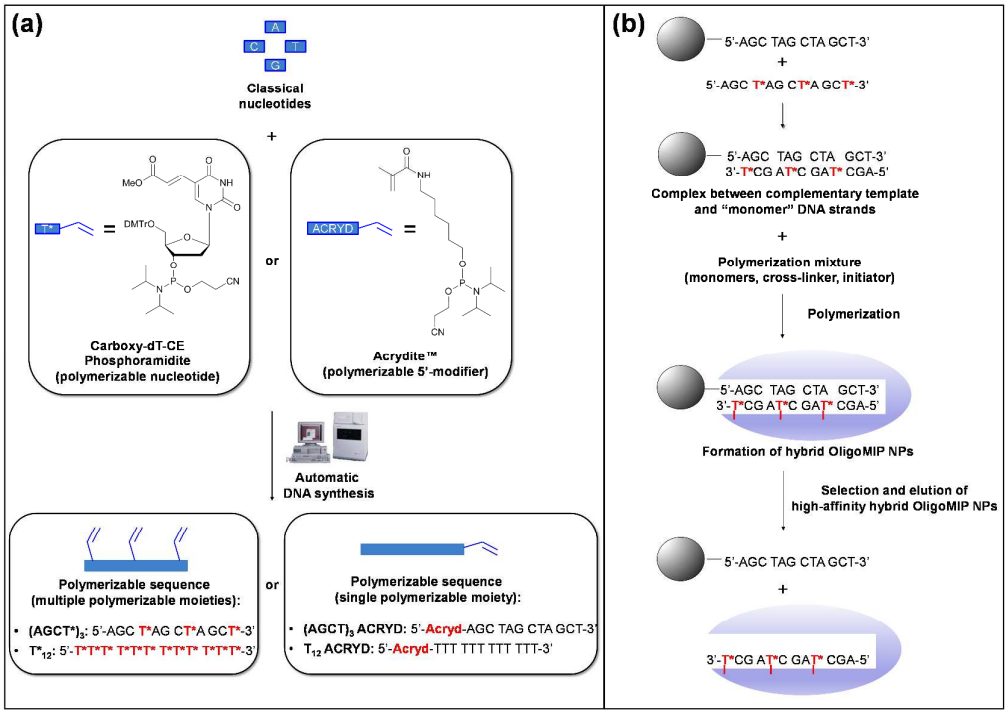

Fig. 2 a) Schematics for the preparation of polymerizable oligonucleotide sequences used as recognition elements in the MIP NPs composition. Polymerizable sequences bear either a single polymerizable moiety through Acrydite™ 5'-modifier (marked as "ACRYD") or several polymerizable moieties through C-5 alkene 2'-deoxyuridine modifications (indicated as "T*"). b) Schematic representation of the solid-phase synthesis and selection of OligoMIP NPs. The polymerizable sequence is incubated first with the solid phase bearing the oligonucleotide template. After this step the remaining classical monomers are added to the solid phase bearing at this point the complex between the complementary DNA strands, and the polymerization is initiated. Low-affinity NPs and unreacted monomers are washed at relatively low temperature (20 °C) using PBS (0.005 M, pH 7.4). The temperature is then increased (60 °C) and high-affinity MIP NPs are eluted from the solid phase using water.

These anchoring points allow the oligonucleotides to participate in the subsequent radical polymerization process: indeed, once both the template and the recognition oligonucleotide are in equilibrium, additional monomers and cross-linkers are added and the polymerization is initiated. After polymerization, unreacted monomers and any low-affinity nanoparticles are washed away, then the high-affinity nanoparticles are eluted at higher temperature and reduced ionic strength (Fig. 2b).[11, 12, 13, 16]

We tested several modified oligonucleotide and control sequences (Fig. 2a), achieving in all cases an incorporation level achieved for the oligonucleotide sequences into the MIP NPs of ~70% (w/w) of the initial feed ratio. Plain MIP NPs have also been prepared for comparison purposes by imprinting the immobilized oligonucleotide template without introducing any DNA monomer in the preparation. In all cases the immobilized oligonucleotide was 5'-AGC TAG CTA GCT-3'.

The Acrydite™ modification can only be incorporated at the 5'-terminal end of the oligonucleotide sequence, whilst the C-5 alkene-modified 2'-deoxyuridine residues can provide multiple anchoring points between the DNA strand and the MIP matrix (Fig. 2). This should allow the oligonucleotide to be held firmly into the cross-linked polymer matrix, thus favoring the best possible recognition performance. Moreover, another advantage of this "nucleotide" modification strategy in comparison to the Acrydite™ method is that the frequency and the location of base modifications could be entirely tailor-made as needed. In this work we only modified dU residues, but there are other examples in the literature in which polymerizable moieties have been introduced on other nucleotides as well.[17]

Dynamic light scattering (DLS) analysis reported hydrodynamic diameter values ranging from 10 nm to 33 nm (Table 1).

Table 1. Particle size distribution and Zeta potential analyses of Plain and OligoMIP NPs in PBS 0.1 M at pH 7.4. Error bars represent ±1 SD (n = 3).

Type of MIP NPs	Particle radius (nm)	Zeta potential (mV)
Plain	11.6 ± 0.5	-10.5 ± 0.3
T_{12} ACRYD	5.1 ± 0.3	-5.8 ± 0.3
T^*_{12}	16.6 ± 0.6	-24.5 ± 0.7
$(AGCT)_3$ ACRYD	9.6 ± 3.4	-9.0 ± 0.3
$(AGCT^*)_3$	16.2 ± 2.5	-13.4 ± 1.0

These data are consistent with the transmission electron microscopy (TEM) analysis (taking into account the swelling in aqueous medium), which showed that OligoMIP NPs appeared spheroidal in shape with their size ranging between 5-15 nm (Fig. 3). Looking at the DLS data more in detail, in relation to the Plain MIP NPs, we can observe that the incorporation of ACRYD modified oligonucleotides [T_{12} ACRYD and $(AGCT)_3$ ACRYD]

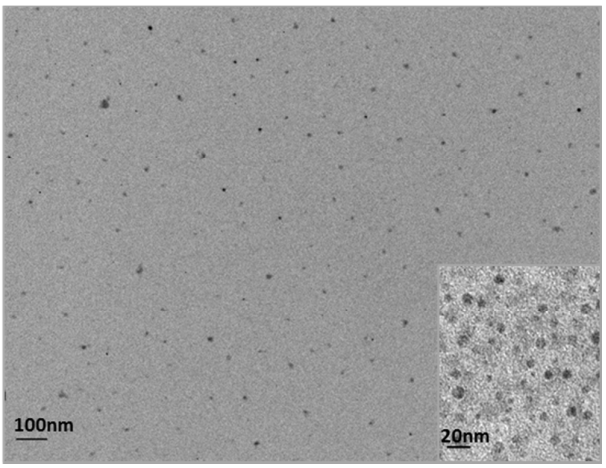

Fig. 3 Transmission Electron Microscopy (TEM) image of $(AGCT^*)_3$ MIP NPs at 30000× magnification. Inset details the spheroidal shape and regular size distribution of the OligoMIP NPs (80000× magnification).

resulted in slightly smaller NPs sizes, whereas incorporation of the modified deoxyuridine-containing oligonucleotides [T^*_{12} and $(AGCT^*)_3$] led to slightly larger OligoMIP NPs (Table 1).

We hypothesize that the changes observed in the particle diameter might depend on the different modification of the oligonucleotide sequences. Specifically, since the Acrydite™ modification possesses more of a hydrophobic character due to the introduction of a C_6 carbon chain at the end of the DNA sequence in comparison to the C-5 alkene deoxyuridine modification, this could result in a more "compact" conformation and smaller size in buffer solution.

This hypothesis seems to be supported by the Zeta potential data (Table 1), according to which the T^*_{12} and $(AGCT^*)_3$ OligoMIP NPs exhibited a more negative Zeta potential value than Plain MIP NPs, which appears to indicate that these oligonucleotide monomers may contribute to the stabilization of the MIP NPs dispersions. On the other hand, T_{12} ACRYD and $(AGCT)_3$ ACRYD OligoMIP NPs exhibited a less negative or more similar Zeta potential value in comparison to Plain MIP NPs, which might indicate that these oligonucleotide monomers could either destabilize or not exhibit an effect on the MIP NPs dispersions.

The MIP NPs produced were then analyzed for their template recognition performance by quartz crystal microbalance (QCM) microgravimetric analysis.[12, 13, 18] The $(AGCT)_3$ oligonucleotide template [or a polyA 12mer (A_{12}) control sequence] was immobilized onto the gold crystal surface using comparable

immobilization conditions as the ones exploited on the solid phase used during imprinting. This is to ensure that the DNA template orientation during rebinding is the same as during the production process of the MIP NPs.

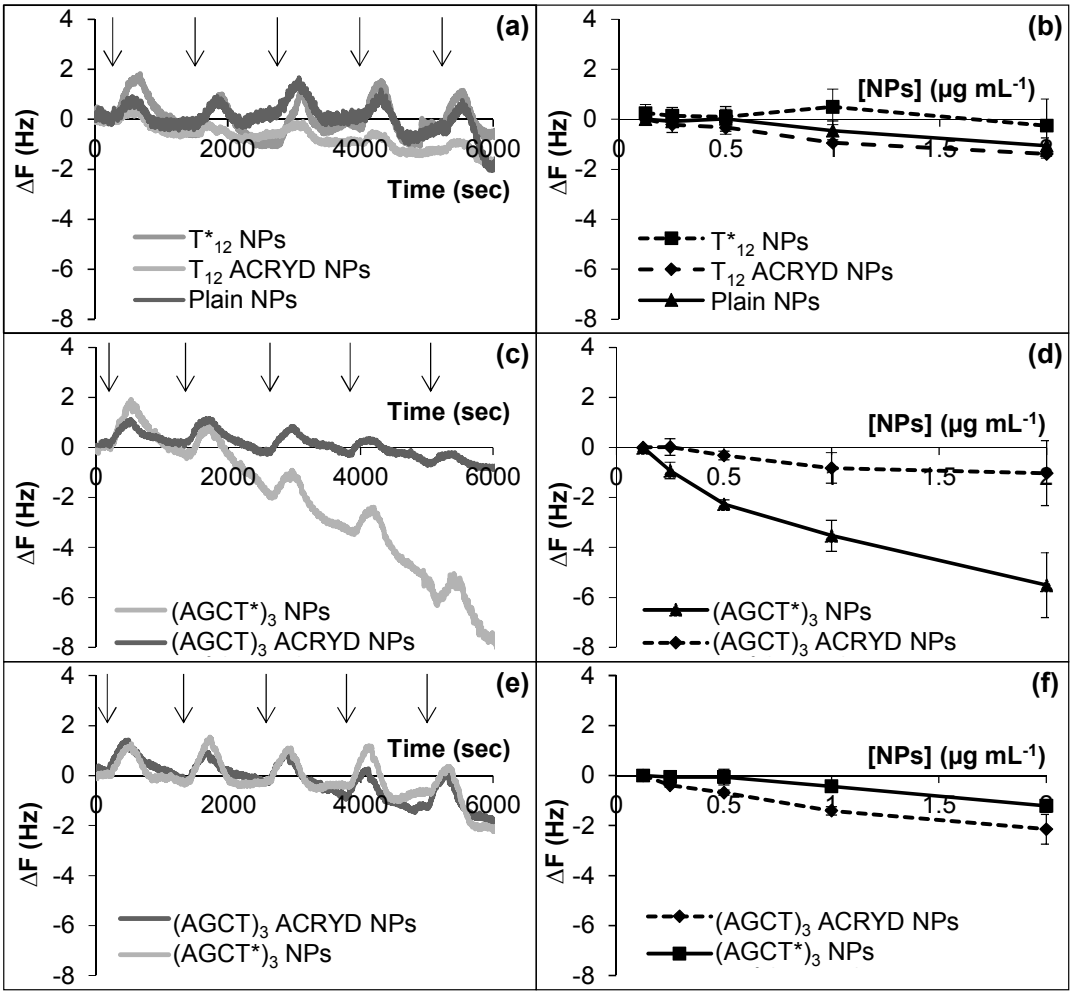

Fig. 4 Rebinding analysis by QCM to template $(AGCT)_3$ and control (A_{12}) derivatized gold surfaces: (a) a typical QCM sensorgram obtained by rebinding different control MIP NPs (Plain, T_{12} ACRYD, and T^*_{12} MIP NPs) to $(AGCT)_3$ oligonucleotide; (b) rebinding performance of control NPs (Plain, T_{12} ACRYD, and T^*_{12} MIP NPs) to $(AGCT)_3$; (c) a typical QCM response obtained by rebinding $(AGCT)_3$ ACRYD MIP NPs and $(AGCT^*)_3$ MIP NPs to the complementary $(AGCT)_3$ oligonucleotide; (d) rebinding performance of $(AGCT)_3$ ACRYD and $(AGCT^*)_3$ MIP NPs to the complementary $(AGCT)_3$ oligonucleotide; (e) a typical QCM sensorgram obtained by injecting $(AGCT)_3$ ACRYD and $(AGCT^*)_3$ MIP NPs onto a A_{12} functionalized gold surface; (f) rebinding performance of $(AGCT)_3$ ACRYD and $(AGCT^*)_3$ MIP NPs to A_{12} oligonucleotide. Drop in frequency (on the Y-axis) indicates the binding event of the MIP NPs to the surface-immobilized oligonucleotide sequence. Arrows indicates the point of injection. A baseline stability value of ±0.2 Hz has been reached between injections. The temporary increase in frequency immediately after the injection point is an artifact due to the pressure variation caused by the injection itself. QCM measurements were performed in PBS (0.03 M, pH 7.4) at 20 °C for the NPs concentrations from 0.125 to 2 μg mL^{-1}. Error bars represent ±1 SD (n = 3).

Several concentrations (from 0.125 to 2 μg mL^{-1}) of the high-affinity fraction of OligoMIP NPs [$(AGCT^*)_3$, $(AGCT)_3$ ACRYD, T^*_{12}, T_{12} ACRYD], or Plain MIP NPs were sequentially flowed (from the lowest to the highest concentration) on the gold crystal bearing the template or the control sequence, and their binding behaviour was recorded. The results of these analyses are detailed in Fig. 4. The QCM sensorgrams indicated that the Plain, T_{12} ACRYD and T^*_{12} MIP NPs (Fig. 4a and 4b) did not exhibit significant binding when tested against QCM crystals bearing the $(AGCT)_3$ template. None of these nanoparticles contained the complementary polymerizable oligomer.

We have previously observed in other contexts that Plain MIP NPs could show an imprinting effect thanks solely to the "classical" monomers, though the addition of a specific monomer (T*) resulting in an improved rebinding performance towards the nucleoside dA template.[12] However, in the case of the oligonucleotide recognition in this study, the Plain MIP NPs exhibited no measurable imprinting effect, showing that classical monomers may lack sufficiently complex moieties to imprint an oligonucleotide sequence.

Moreover, inclusion of a non-complementary oligonucleotide (T_{12} ACRYD and T^*_{12} MIP NPs, Fig. 4a and 4b) did not help with the imprinting. Thus the binding observed for complementary sequences is not simply related to the presence of a polymerizable oligonucleotide in the imprinting mixture.

Interestingly, even when the complementary $(AGCT)_3$ was incorporated through a 5'-Acrydite™ modification [$(AGCT)_3$ ACRYD MIP NPs], it exhibited very poor recognition performance (Fig. 4c and 4d). In contrast, the MIP NPs in which the DNA modification strategy involved multiple anchoring points [$(AGCT^*)_3$ MIP NPs] showed excellent binding behaviour (Fig. 4c and 4d). This suggests that multi-point incorporation, which may preorganize the oligonucleotide conformation into an appropriate helical structure, is significantly more effective at developing nanoparticles with appropriate binding cavities for their targets.

To further explore these results, we took the "active" nanoparticles which showed strong binding to $(AGCT)_3$, [$(AGCT)_3$ ACRYD and $(AGCT^*)_3$ MIP NPs] and tested them for binding to another immobilized strand, A_{12} (Fig. 4e and 4f).

The sensorgrams are comparable to the binding levels observed by the non-specific NPs shown in Fig. 4b. This suggests that none of the $(AGCT)_3$ OligoMIP NPs bound to the non-complementary A_{12} sequence, thus confirming that the specific binding event observed in the case of $(AGCT^*)_3$ MIP NPs requires the presence of the correct complementary DNA sequence in an imprinted matrix.

Experimental

Materials

N-isopropylacrylamide (NIPAm), *N,N,N',N'*-tetra-methylethylenediamine (TEMED), ammonium persulphate (APS), acrylic acid (AAc), *N,N'*-methylenebisacrylamide (BIS), *N-tert*-butylacrylamide (TBAm), 3-aminopropyltriethyloxy-silane (APTES), cysteamine, glass beads, SPE cartridges and frits, toluene, methanol and acetone were purchased from Sigma-Aldrich (UK). Sodium hydroxide, sulfuric acid, 1-ethyl-3-(3-dimethylaminopropyl)carbodiimide (EDC), imidazole, ethylenediaminetetraacetic acid (EDTA) and phosphate buffered saline (PBS) were purchased from Fisher Scientific (UK). Ethanol and hydrogen peroxide were purchased from VWR (UK). DNA sequences bearing the Acrydite™ and Phosphate (Phos) modification were purchased from Integrated DNA Technologies, Inc (USA). Carboxy-dT-CE Phosphoramidite was purchased from Link (UK). Double-distilled water (Millipore) was used for analysis. All chemicals and solvents were analytical or HPLC grade and were used without further purification.

Synthesis of polymerizable oligomer sequences [T^*_{12}, $(AGCT^*)_3$]

Oligonucleotides were synthesized under standard conditions at 1 µmol scale on an Applied Biosystems 394 oligonucleotide synthesizer. The oligomers were deprotected and released from the support by treatment with concentrated aqueous NH_3 at 55 °C for 16 h. The solutions were concentrated to dryness, resuspended in water and desalted using NAP-10 columns (GE Healthcare). Oligonucleotide masses were verified using a Bruker micrOTOF LCMS system.

Preparation of $(AGCT)_3$-derivatized glass beads as affinity media

Glass beads (125 g, 75 µm diameter, Supelco) were activated by boiling in NaOH (1 M) for 10 min, then washed thoroughly with double-distilled water at 60 °C, acetone and finally dried at 80 °C. They were then incubated in a solution of APTES (2 %, v/v) in anhydrous toluene overnight at room temperature, then washed with acetone and dried under vacuum. The 5'-Phos-AGC TAG CTA GCT-3' template sequence (425 nmol) was activated in 283 µL PBS (0.01 M, EDTA 0.01 M, pH 7.2) by adding 40 µL EDC and immediately transferring this solution into 22.5 g of APTES-derivatized glass beads suspended in 10 mL of imidazole buffer (0.1 M, pH 6.0). The glass beads were incubated with the DNA template for 2 h at 50 °C and then overnight at room temperature (0.67 mL solution/g glass beads). The derivatized beads were washed thoroughly with double-distilled water and dried under vacuum. After this step the glass beads were used straight away for the synthesis of the MIP NPs without further storage. The immobilization of the template was confirmed spectrophotometrically (at λ = 260 nm) by analyzing the amount of DNA unbound to the glass beads and found in the washings collected from the immobilization step.

Solid-phase synthesis of Plain and OligoMIP NPs

A solution (2.5 mL) of each polymerizable DNA oligomer sequence in PBS (0.005 M, pH 7.4) was degassed by purging with Ar for 10 min and then incubated for 1 h at room temperature in a 14 mL glass vial closed using a Teflon screw-cap and containing 5 g of $(AGCT)_3$-derivatized glass beads (0.67 mL solution/g glass beads), for a total of five polymerization vials [Plain MIP NPs, T_{12} ACRYD MIP NPs, $(AGCT)_3$ ACRYD MIP NPs, T^*_{12} MIP NPs, $(AGCT^*)_3$ MIP NPs]. In the case of Plain MIP NPs, 2.5 mL of PBS were added to maintain the incubation conditions similar to the other samples. Prior to the addition of the oligomer solutions, the vials containing the solid phase were degassed under vacuum and the air inside the vials then replaced with Ar (3 times). In the meantime the following monomers were dissolved in PBS (0.005 M, pH 7.4, 50 mL): NIPAm (39 mg, 0.35 mmol, 53%), BIS (2 mg, 0.01 mmol, 2%), TBAm (33 mg, 0.26 mmol, 40%) and AAc (2.2 µL, 0.03 mmol, 5%). TBAm was previously dissolved in EtOH (1 mL) and then added to the aqueous solution. The total monomer concentration was 13 mM at this stage. The solution was degassed under vacuum and sonication for 10 min, and then purged with Ar for 30 min. After this time, aliquots of 2.5 mL of solution were transferred in the vials previously incubated with the polymerizable DNA, thus reaching a total volume of 5 mL and a final monomer concentration of 6.5 mM. The polymerization was started by adding an APS aqueous solution (50 µL, 60 mg mL^{-1}) and TEMED (1.5 µL). The polymerization was then carried out at 20 °C for 20 h. After the polymerization, the contents of the vials were transferred into SPE cartridges fitted with a polyethylene frit (20 µm porosity) in order to perform the temperature-based affinity separation of MIP NPs. The temperature of PBS and the SPE cartridges was kept at 20 °C (same as the polymerization step). Washing

was performed with 3 × 5 mL of PBS (0.005 M, pH 7.4), applying manual pressure with a syringe if needed. This was done in order to remove non-polymerized monomers and low-affinity MIP NPs. The effectiveness of the washing was verified by measuring the UV absorbance of washing aliquots, in order to ensure complete monomer removal as well as to quantify the incorporation of polymerizable DNA into the polymer matrix (by difference of the absorbance measured at λ = 260 nm). Afterwards the SPE cartridges containing the solid phase with high-affinity MIP NPs attached were heated up to 60 °C and eluted with 5 × 5 mL H_2O at 60 °C. The concentration of the nanoparticles fractions has been evaluated by evaporation.

Transmission Electron Microscopy (TEM) analysis

TEM images of MIP NPs were taken using a JEOL JEM 1400, 120kV high contrast TEM equipped with an AMT XR60 mid-mount digital camera (11 megapixels). Samples for the analysis were prepared by depositing a drop of the MIP NPs solution, previously filtered through a 0.45 µm PTFE syringe filter, on a carbon-coated TEM copper grid (300 mesh, from Agar Scientific, UK), blotting away the excess and leaving them to dry overnight at room temperature.

Dynamic Light Scattering (DLS) analysis

The MIP NPs samples for DLS were prepared in deionized H2O, sonicated for 5 minutes, then filtered through 0.45 µm PTFE syringe filters and analyzed in Quartz SUPRASIL (1.5 × 1.5 mm) cuvette at 25 °C by using Malvern Viscotek DLS (Malvern Instruments Ltd.) equipped with OMNISIZE 3.0 software.

Zeta Potential analysis

The MIP NPs were dispersed in PBS (10 mM, pH 7.4) and transferred to DTS1060C clear disposable 1 mL zeta flow-cells. The analysis was done on Malvern Zetasizer Nano Z (Malvern Instruments Ltd.) using the Smoluchowski model.

Treatment of Quartz Crystal Microbalance (QCM) crystals and surface immobilization of templates

QCM crystals (5 MHz Cr/Au, polished, Testbourne Ltd., UK) were cleaned by immersion in Piranha solution (H_2SO_4/H_2O_2, 3/1, v/v) for 5 min. **Caution! This mixture is highly corrosive; hence extreme care is required during this process.** Then they were thoroughly rinsed with double-distilled water and left in MeOH overnight. The immobilization of the templates has been performed by incubating the crystals in a solution of cysteamine (0.2 mg mL^{-1}) in EtOH at 4 °C for 24 h, after which they have been washed with EtOH and incubated for at least 48 h at room temperature in a 10 mL solution of 5'-Phos-AGC TAG CTA GCT-3' template sequence (425 nmol) in imidazole buffer (0.1 M, pH 6.0). The template was previously activated in 283 µL PBS (0.01 M, EDTA 0.01 M, pH 7.2) by adding 40 µL EDC (same activation as for the immobilization onto the glass beads). Once the immobilization was completed, the crystals were washed thoroughly with double-distilled water before being mounted in the QCM flowcell.

QCM microgravimetric analysis of Plain and OligoMIP NPs

Plain and OligoMIP NPs adsorption to the $(AGCT)_3$ template was monitored using a QCM200 5 MHz quartz crystal microbalance (Stanford Research Systems, UK). The modified QCM chips were maintained hydrated during mounting in the QCM flowcell. MIP NPs solutions and running buffer were introduced using an Instech P720 peristaltic pump equipped with 0.020" ID tubing (Linton Instrumentation, UK) and flowing at 0.1 µL min^{-1}. The QCM chip bearing the template was first stabilized in running buffer (PBS 0.003 M, pH 7.4) at 20 °C until the system reached a stable baseline. Affinity analysis was carried out by sequentially by flowing each MIP NPs solution for 5 min (500 µL) and analyzing the sensor response for 15 min. This process was repeated over the concentration range of 0.125-2 µg mL^{-1}.

Conclusions

In conclusion, hybrid OligoMIP NPs were successfully produced for a model oligomer DNA sequence (5'-AGC TAG CTA GCT-3') by exploiting a modified oligonucleotide bearing multiple polymerizable moieties as a tailored functional monomer. Nanoparticles were obtained using a solid-phase imprinting polymerization strategy in which template-derivatized glass beads double as an affinity matrix for production as well as selection and purification of synthesized MIP NPs.

The physical analysis of OligoMIP NPs showed narrow particle size distributions and spheroidal shapes, with a size comparable to natural antibodies.[19]

QCM microgravimetric analysis of the synthesized OligoMIP NPs confirmed that maximum specificity and selectivity are achieved only when the correct complementary DNA sequence is structurally supported and locked in position into the MIP matrix by multiple anchoring points provided by the polymerizable nucleotides. It is hypothesized that the use of a single anchor point allowed the DNA structure entrapped within the polymer to alter shape and hence be unviable as a target site, whereas the multiple point binding fixed the sequence in place. This is supported by previous observations.[13]

Such OligoMIP nanosystems could potentially be applied for the development of biosensors or even in vivo therapeutics and diagnostics. [4, 20] Our previous work on aptamer-functionalized MIPs showed that imprinting conferred a very high level of nuclease stability on the oligonucleotide, giving significant advantages when working in biological contexts.[13] We are currently investigating the possibility of using these materials for these and other applications.

Acknowledgements

The authors would like to acknowledge the financial support of The Open University and of Engineering and Physical Sciences Research Council (EPSRC) for the award of a First Grant (EP/K015095/1). We also thank Mrs. Heather Davies for the

help with the TEM imaging and Prof. Cameron Alexander for the help with the DLS and Zeta potential measurements. We thank ATD Bio for access to the oligonucleotide synthesizer used in this work.

Notes and references

1 E. T. Kool, *Chem. Rev.*, 1997, **97**, 1473-1488; M. Petersen and J. Wengel, *Trends Biotechnol.*, 2003, **21**, 74-81; R. N. Veedu and J. Wengel, *RNA Biol.*, 2009, **6**, 321-323; J. S. Jepsen, M. D. Sorensen and J. Wengel, *Oligonucleotides*, 2004, **14**, 130-146; J. K. Watts, *Chem. Commun. (Camb.)*, 2013, **49**, 5618-5620.

2 2D. P. Bartel, *Cell*, 2009, **136**, 215-233; Y. Tomari and P. D. Zamore, *Genes Dev.*, 2005, **19**, 517-529.

3 N. W. Turner, C. I. Holdsworth, S. W. Donne, A. McCluskey and M. C. Bowyer, *New J. Chem.*, 2010, **34**, 686-692.

4 Y. Hoshino, H. Koide, K. Furuya, W. W. Haberaecker, 3rd, S. H. Lee, T. Kodama, H. Kanazawa, N. Oku and K. J. Shea, *Proc. Natl. Acad. Sci. U. S. A.*, 2012, **109**, 33-38.

5 Y. Wang, Z. Zhang, V. Jain, J. Yi, S. Mueller, J. Sokolov, Z. Liu, K. Levon, B. Rigas and M. H. Rafailovich, *Sensors Actuators B: Chem.*, 2010, **146**, 381-387; S. Wang, J. Ye, Z. Bie and Z. Liu, *Chem. Sci.*, 2014, **5**, 1135-1140.

6 I. Bacskay, A. Takatsy, A. Vegvari, A. Elfwing, A. Ballagi-Pordany, F. Kilar and S. Hjerten, *Electrophoresis*, 2006, **27**, 4682-4687; Z. Zhang, Y. Guan, M. Li, A. Zhao, J. Ren and X. Qu, *Chem. Sci.*, 2015, **6**, 2822-2826; K. Ren and R. N. Zare, *ACS Nano*, 2012, **6**, 4314-4318; M. Mahmoudi, S. Bonakdar, M. A. Shokrgozar, H. Aghaverdi, R. Hartmann, A. Pick, G. Witte and W. J. Parak, *ACS Nano*, 2013, **7**, 8379-8384.

7 K. Haupt, *Nat Mater*, 2010, **9**, 612-614; A. Poma, A. P. F. Turner and S. A. Piletsky, *Trends Biotechnol.*, 2010, **28**, 629-637; A. Poma, M. J. Whitcombe and S. Piletsky, in *Designing Receptors for the Next Generation of Biosensors*, eds. S. Piletsky and M. J. Whitcombe, Springer-Verlag Berlin Heidelberg, Berlin, First edn., 2013, ch. 6, pp. 105-130.

8 Y. Hoshino, R. C. Ohashi and Y. Miura, *Adv. Mater.*, 2014, **26**, 3718-3723; Z. Zeng, Y. Hoshino, A. Rodriguez, H. Yoo and K. J. Shea, *ACS Nano*, 2010, **4**, 199-204.

9 N. O. Aouled, H. Hallil, B. Plano, D. Rebiere, C. Dejous, R. Delepee and L. Agrofoglio, *SENSORS, 2013 IEEE*, 2013, 1-4; A. Krstulja, S. Lettieri, A. J. Hall, R. Delepee, P. Favetta and L. A. Agrofoglio, *Anal. Bioanal. Chem.*, 2014, **406**, 6275-6284; O. Slinchenko, A. Rachkov, H. Miyachi, M. Ogiso and N. Minoura, *Biosens. Bioelectron.*, 2004, **20**, 1091-1097.

10 R. M. Garcinuno, I. Chianella, A. Guerreiro, I. Mijangos, E. V. Piletska, M. J. Whitcombe and S. A. Piletsky, *Soft Matter*, 2009, **5**, 311-317.

11 A. Poma, A. Guerreiro, S. Caygill, E. Moczko and S. Piletsky, *RSC Advances*, 2014, **4**, 4203-4206; A. Poma, A. Guerreiro, M. J. Whitcombe, E. V. Piletska, A. P. F. Turner and S. A. Piletsky, *Adv. Funct. Mater.*, 2013, **23**, 2821-2827.

12 A. Poma, H. Brahmbhatt, J. K. Watts and N. W. Turner, *Macromolecules*, 2014, **47**, 6322–6330.

13 A. Poma, H. Brahmbhatt, H. M. Pendergraff, J. K. Watts and N. W. Turner, *Adv. Mater.*, 2015, **27**, 750-758.

14 G. T. Hermanson, *Biocojugate Techniques*, Academic Press, London, 3rd edn., 2013.

15 J. Liu, *Soft Matter*, 2011, **7**, 6757-6767; N. Dave, M. Y. Chan, P. J. Huang, B. D. Smith and J. Liu, *J. Am. Chem. Soc.*, 2010, **132**, 12668-12673; Y. H. Roh, R. C. Ruiz, S. Peng, J. B. Lee and D. Luo, *Chem. Soc. Rev.*, 2011, **40**, 5730-5744; T. J. Bandy, A. Brewer, J. R. Burns, G. Marth, T. Nguyen and E. Stulz, *Chem. Soc. Rev.*, 2011, **40**, 138-148.

16 A. Guerreiro, A. Poma, K. Karim, E. Moczko, J. Takarada, I. P. de Vargas-Sansalvador, N. Turner, E. Piletska, C. S. de Magalhaes, N. Glazova, A. Serkova, A. Omelianova and S. Piletsky, *Adv. Healthc. Mater.*, 2014, **3**, 1426–1429; E. Moczko, A. Poma, A. Guerreiro, I. Perez de Vargas Sansalvador, S. Caygill, F. Canfarotta, M. J. Whitcombe and S. Piletsky, *Nanoscale*, 2013, **5**, 3733-3741.

17 W. Xu, J. G. Wang, M. F. Jacobsen, M. Mura, M. Yu, R. E. Kelly, Q. Q. Meng, E. Laegsgaard, I. Stensgaard, T. R. Linderoth, J. Kjems, L. N. Kantorovich, K. V. Gothelf and F. Besenbacher, *Angew. Chem. Int. Ed. Engl.*, 2010, **49**, 9373-9377; V. B. Pinheiro and P. Holliger, *Curr. Opin. Chem. Biol.*, 2012, **16**, 245-252; L. N. Burgula, K. Radhakrishnan and L. M. Kundu, *Tetrahedron Lett.*, 2012, **53**, 2639-2642; X. Zhang, J. Wang and Y. Z. Xu, *Magn. Reson. Chem.*, 2013, **51**, 523-529.

18 N. W. Turner, B. E. Wright, V. Hlady and D. W. Britt, *J. Colloid Interface Sci.*, 2007, **308**, 71-80.

19 M. Reth, *Nat. Immunol.*, 2013, **14**, 765-767.

20 Y. Ben-Amram, R. Tel-Vered, M. Riskin, Z.-G. Wang and I. Willner, *Chem. Sci.*, 2012, **3**, 162-167; I. Chianella, A. Guerreiro, E. Moczko, J. S. Caygill, E. V. Piletska, I. M. P. De Vargas Sansalvador, M. J. Whitcombe and S. A. Piletsky, *Anal. Chem.*, 2013, **85**, 8462-8468; R. V. Shutov, A. Guerreiro, E. Moczko, I. P. de Vargas-Sansalvador, I. Chianella, M. J. Whitcombe and S. A. Piletsky, *Small*, 2014, **10**, 1086-1089; S. Carrasco, E. Benito-Pena, D. R. Walt and M. C. Moreno-Bondi, *Chem. Sci.*, 2015, **6**, 3139-3147.